

## Acceleration-based neural networks algorithm for damage detection in structures

Jeong-Tae Kim\* and Jae-Hyung Park<sup>‡</sup>

*Department of Ocean Engineering, Pukyong National University, Nam-gu, Busan 608-737, Korea*

Ki-Young Koo<sup>‡†</sup>

*Department of Civil & Environmental Engineering, Korea Advanced Institute of Science & Technology, Daejeon, Korea*

Jong-Jae Lee<sup>‡‡</sup>

*Department of Civil & Environmental Engineering, Sejong University, Seoul, Korea*

*(Received August 15, 2007, Accepted March 3, 2008)*

**Abstract:** In this study, a real-time damage detection method using output-only acceleration signals and artificial neural networks (ANN) is developed to monitor the occurrence of damage and the location of damage in structures. A theoretical approach of an ANN algorithm that uses acceleration signals to detect changes in structural parameters in real-time is newly designed. Cross-covariance functions of two acceleration responses measured before and after damage at two different sensor locations are selected as the features representing the structural conditions. By means of the acceleration features, multiple neural networks are trained for a series of potential loading patterns and damage scenarios of the target structure for which its actual loading history and structural conditions are unknown. The feasibility of the proposed method is evaluated using a numerical beam model under the effect of model uncertainty due to the variability of impulse excitation patterns used for training neural networks. The practicality of the method is also evaluated from laboratory-model tests on free-free beams for which acceleration responses were measured for several damage cases.

**Keywords:** artificial neural network; output-only acceleration; real-time damage detection; structural health monitoring.

---

### 1. Introduction

Structural health monitoring has become the important research topic for securing the safety of infrastructures. Vibration-based damage assessment is an important sub-problem related to structural health monitoring. Many researchers have focused on developing reliable vibration-based techniques that use

\*Professor, E-mail: [idis@pknu.ac.kr](mailto:idis@pknu.ac.kr)

<sup>‡</sup>Ph.D. Student

<sup>‡†</sup>Postdoctoral Researcher

<sup>‡‡</sup>Assistant Professor

vibration characteristics of a structure to detect, locate and size the damage in the structure. A vibration-based damage detection system can not be suitable for practical applications until it can accurately acquire structural response signals, extract physically useful information from the signals, and utilize the feature information for damage detection and structural assessment (Chen and Feng 2005, Catbas and Aktan 2002, Doebling and Farrar 1998, Kim and Stubbs 1995).

Up-to-date, vibration-based damage detection methods are implemented by a series of signal acquisition, data analysis in time and frequency domains, pattern recognition and system identification process. In order to fulfill the existing damage detection methods which are either signal-based or model-based methods, at least three significant amounts of works are needed: (1) to obtain acceleration-response signals measured at selected multiple locations, (2) to extract modal parameters such as natural frequencies and mode shapes from the signals, and (3) to modify the measured modal information suitable for certain damage detection algorithms such as damage index methods, genetic algorithm (GA)-based methods, and artificial neural networks (ANN)-based methods (Kim, *et al.* 2003, Hao and Xia, 2002, Kim, *et al.* 2007, Lee, *et al.* 2005, Ni, *et al.* 2002).

Recently, ANN algorithms have been studied for vibration-based damage detection due to the advantage in dealing with various types of input and output and the efficient pattern-recognition capability with various training patterns. Many researchers have made efforts to develop ANN techniques for identifying the location and the extent of damage (Wu, *et al.* 2001, Jang and Imregun, 2001, Szewczyk and Hajela, 1994), to develop a substructural identification method for complex structures using multilayer perceptron (Yun and Bhang 2001), to implement the ANN techniques using modal data to health monitoring of bridges (Lee, *et al.* 2005, Ni, *et al.* 2002, Lee, *et al.* 1999, Barai and Pandey 1995).

However, several problems still remain to be resolved before the ANN techniques can be successfully implemented for damage detection in large structures. Most of signal process and modal analyses need off-line works that are time-consuming depending on the number of sensors involved and the amount of signals recorded. Also, errors in baseline FE models cause errors in modal parameters used for the input of neural networks and those errors have effects on the accuracy of damage detection. The error in the baseline model is critical since modal parameters are to be generated for various perturbed cases of the baseline model and used as training patterns for the neural networks. Those problems hinder the implementation of on-line damage monitoring into real structures. For the realization of the on-line health monitoring, therefore, it is needed to develop a damage detection method that uses real-time signals measured from a limited number of sensors, without any further frequency-domain data-process, to identify the changes in structural conditions (Gao and Spencer 2002, Kim, *et al.* 2006, Yang *et al.* 2007).

In this study, a real-time damage detection method using output-only acceleration signals and artificial neural networks (ANNs) is developed to monitor the occurrence of damage and its location in structures. In order to achieve the objective, the following approaches are used. Firstly, theoretical backgrounds are described. The problem addressed in this paper is defined as the stochastic process. An ANN-algorithm that uses output-only acceleration responses to detect changes in structural parameters in real-time is newly designed. As the feature representing the structural condition, we select the cross-covariance function of two acceleration-signals measured at two different locations. By means of the acceleration features, a set of neural networks are trained for a series of potential loading patterns and damage scenarios of the target structure for which its actual loading histories and structural conditions are unknown. The feasibility of the proposed method is evaluated from numerical tests on a simply supported beam model under the effect of model uncertainty due to the variability of impulse excitation patterns used for training neural networks. The practicality of the method is also evaluated from

laboratory-model tests on free-free beams for which a series of accelerations were measured for several damage cases.

## 2. Theoretical backgrounds

### 2.1 Problem statement

The problem addressed here may be defined as follows: Given a structural system that exhibits the stochasticity in some physical parameters and a set of the dynamic responses of that structural system; then estimate the physical parameters by knowing the dynamic responses (Bendat and Piersol 1991). Here the parameter of interest will be some form of stiffness, e.g., bending or axial. In this paper, the discussion is limited to a broad-band stationary discrete process  $\{X_k(t)\}$ . Each particular function  $X_k(t)$ , where  $t$  is variable and  $k$  is fixed, is a sample function.

For a pair of stationary random processes  $\{X_k(t)\}$  and  $\{Y_k(t)\}$ , the normalized cross-covariance function,  $\rho_{XY}(\tau)$ , is estimated by

$$\rho_{XY}(\tau) = \frac{R_{XY}(\tau) - \mu_X \mu_Y}{\sigma_X \sigma_Y} \quad (1)$$

where  $\mu_X$  and  $\mu_Y$  are the means,  $\sigma_X$  and  $\sigma_Y$  are the standard deviations,  $R_{XY}(\tau)$  is the cross-correlation function between  $\{X_k(t)\}$  and  $\{Y_k(t)\}$ . The function  $\rho_{XY}(\tau)$  measures the linear dependency between  $\{X_k(t)\}$  and  $\{Y_k(t)\}$  for a displacement of  $\tau$  in  $\{Y_k(t)\}$  relative to  $\{X_k(t)\}$ .

### 2.2. Acceleration-based ANN algorithm

Suppose that we are given an arbitrary structure with NE elements and N nodes. By assuming that the structure behaves linearly, the acceleration response vector at a certain time  $t$  for a multi-degree-of-freedom system can be given by

$$\{\ddot{X}_t\} = [M]^{-1}(\{F\} - [C]\{\dot{X}_t\} - [K]\{X_t\}) \quad (2)$$

in which  $[M]$ ,  $[C]$  and  $[K]$  are, respectively, mass, damping and stiffness matrices of the system;  $\{F\}$  is unknown (or unmeasured) excitation force vector; and  $\{X_t\}$ ,  $\{\dot{X}_t\}$ , and  $\{\ddot{X}_t\}$  are, respectively, displacement, velocity, and acceleration response vectors.

As described in Eq. (2), the acceleration response at a certain location changes due to the perturbation of the structural parameters in NE elements. With the known force vector  $\{F\}$ , the patterns of the dynamic responses at a location can be recognized as the consequence of the changes in physical parameters of all other locations in the structure. Consequently, the acceleration responses obtained before and after damage can be used as the input for the ANN-based damage detection. However, this approach is limited only when the external forces that are applied for the real structure is known and identical to the ones that are used for training neural networks. Therefore, the use of the acceleration as the direct input will cause the problem.

As an alternative input, instead, the cross-covariance-ratios between intact and damaged state were selected: 1) to indicate damaged state with respect to the undamaged state and 2) to sense both the location of damage and the amount of damage. A cross-covariance function of two accelerations measured at  $i$ th and  $j$ th locations (which are a pair of stationary random processes  $\ddot{X}_i$  and  $\ddot{X}_j$ ) as

described in Eq. (1) is defined as follows:

$$\rho_{\ddot{X}_i, \ddot{X}_j}(\tau) = \frac{R_{\ddot{X}_i, \ddot{X}_j}(\tau) - \mu_{\ddot{X}_i} \mu_{\ddot{X}_j}}{\sigma_{\ddot{X}_i} \sigma_{\ddot{X}_j}} \quad (3)$$

where  $\mu_{\ddot{X}_i}$  and  $\mu_{\ddot{X}_j}$  are the means;  $\sigma_{\ddot{X}_i}^2$  and  $\sigma_{\ddot{X}_j}^2$  are the variances; and  $R_{\ddot{X}_i, \ddot{X}_j}(\tau)$  is the cross-correlation function between  $\ddot{X}_i$  and  $\ddot{X}_j$ . The function  $\rho_{\ddot{X}_i, \ddot{X}_j}(\tau)$  measures the linear dependency between  $\ddot{X}_i$  and  $\ddot{X}_j$  for a displacement of  $\tau$  in  $\ddot{X}_j$  relative to  $\ddot{X}_i$ . Assuming that impact forces applied in intact state and damaged states are the same, the cross-covariance-ratios could be estimated from cross-covariance functions measured in intact and damaged states.

The networks consist of an input layer, a hidden layer, and an output layer, as shown in Fig. 1. The input/output relationship of the neural networks can be nonlinear, as well as linear, and its characteristics are determined by the synaptic weights assigned to the connections between the neurons in two adjacent layers. A systematic way of updating the weights to achieve a desired input/output relationship based on a set of training patterns is referred to as training or learning algorithm. In this study, the conventional back-propagation algorithm is employed. The input layer contains the measured cross-covariance-ratios,  $\widehat{\rho}_{\ddot{X}_i, \ddot{X}_j}(\tau) / \rho_{\ddot{X}_i, \ddot{X}_j}(\tau)$ , where the cap denotes the damaged state. The output from the neural networks are element's physical properties which represent the fractional changes in mass, damping, and stiffness, as described in Eq. (2). By assuming the mass and damping properties in Eq. (2) are not changed before and after damage, the output layer consists of the element-level stiffness indices to be identified as (Lee, *et al.* 2005)

$$S_j = k_{j,d} / k_{j,u} \quad (4)$$

where  $k$  is element stiffness. Subscript  $j$  denotes an element number such as  $j = 1, 2, \dots, NE$  and subscripts  $u$  and  $d$  denote intact and damaged state, respectively. The element-level damage severity of the  $j$ th element is described as

$$\alpha_j = 1 - S_j \quad (5)$$

The acceleration-based neural networks algorithm is newly schematized as shown in Fig. 2. It consists of two parts: (a) Training neural networks and (b) Alarming damage location using the trained neural networks. Training neural networks (TNN) is performed in the following four steps. Firstly, a baseline finite element (FE) model with  $NE$  elements is selected for the target structure. Secondly,  $N$  numbers of excitation patterns are selected on the basis of potential loading scenarios of the structure. In case of output-only situations (for most of real bridges), it is very difficult to exactly identify the real arbitrary load pattern applied to the structure. It is rather realistic to start with the monitoring system utilizing ideal impact load patterns. An impact load could be modeled by its shape, duration and intensity. Since a loading pattern matching to the real excitation is not possible unless it is measured, multiple loading patterns, one of which is a potential pattern, should be considered as many as possible in order to account for the pattern of the real impact load. Thirdly,  $M$  numbers of damage patterns are decided on the basis of the potential damaging scenarios of the structure. Each damage pattern is characterized by element-level stiffness losses. Finally, a set of multiple neural networks are trained for the  $N$  excitation patterns and the  $M$  damaging patterns. A single neural network could be used to train for the  $N$  excitation patterns and  $M$  damaging patterns. However, a single neural network had the

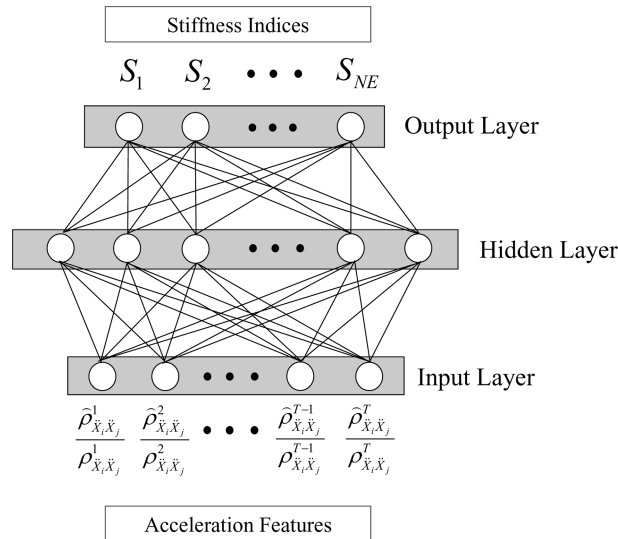


Fig. 1 Architecture of back-propagation neural networks

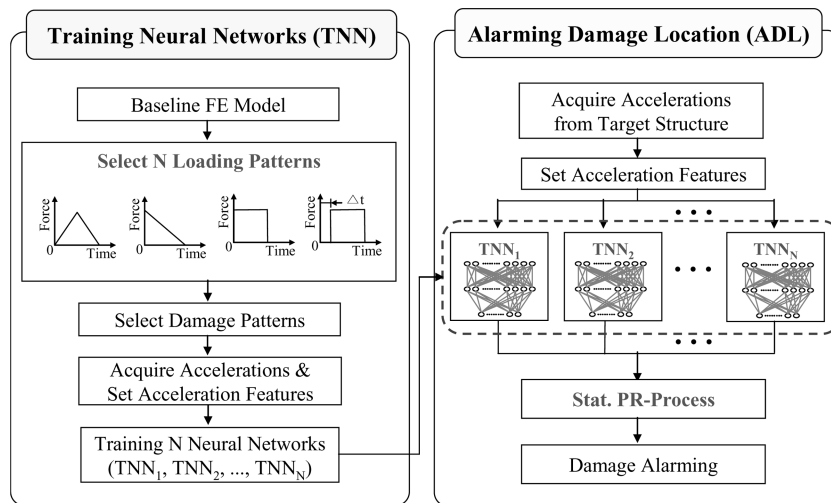


Fig. 2 Schematic of acceleration-based neural networks for damage detection

difficulty, relative to the selected multiple neural networks, in the number of training patterns, the calculation time, and the output convergence under error tolerance.

The cross-covariance values are computed from two acceleration signals measured before and after damage. The ratios of the cross-covariance values between before and after damage are the inputs to the neural networks. Training neural networks is repeated until the  $N$  sets of neural networks are trained for the  $N$  excitation patterns. An individual excitation pattern is trained for an independent set of neural networks. That is, a set of neural networks is corresponding to a specific excitation pattern, which is independent of other excitation patterns.

Alarming damage location (ADL) is performed in the following procedures. Firstly, accelerations are measured at two different locations of the real target structure before and after damage occurred.

Secondly, the ratios of the cross-covariance values of the two accelerations between intact and damaged state is computed and furthermore input into the pre-trained neural networks. Thirdly, element stiffness indices (i.e.  $S_j$  of Eq. 4) and severity indices (i.e.  $\alpha_j$  of Eq. 5) are estimated for  $NE$  output elements from the soft computing process. ADL is repeated for the  $N$  sets of pre-trained neural networks, from which stiffness indices and severity indices are estimated as  $S_{ji}$  and  $\alpha_{ji}$  ( $i = 1, 2, \dots, N$ ,  $j = 1, 2, \dots, NE$ ), respectively.

We realize that the values computed for the damage indices will always contain many uncertainties which may be associated with errors in baseline models, neural networks, acceleration measurements, and data process and information analyses. More specifically, there are uncertainties due to the difference between excitation-force models in neural networks and actual loading conditions of the target structure and also due to the variation resulting from environmental fluctuation during the test. It follows that before damage is assigned to any element, these uncertainties should be addressed. Here, a statistical-based method is used to assign damage to an element by accounting for the impact of these uncertainties.

To account for all available  $N$  sets of neural networks (i.e. the  $N$  sets of excitation patterns) we form a single indicator (DI) for the  $j$ th element as (Kim, *et al.* 2003):

$$DI_j = \left( \sum_{i=1}^N \alpha_{ji}^2 \right)^{1/2} \quad (6)$$

where  $0 \leq DI_j \leq \infty$  and the damage is located at element  $j$  if  $DI_j$  approaches the local maximum point.

A set of stiffness indices that correspond to a set of neural networks has been treated as random variables. To classify those indices into one of two spaces (undamaged or damage), a pattern classification algorithm has been implemented in three steps: 1) to obtain  $N$  sets of damage indices corresponding to  $N$  sets of neural networks, 2) to assemble damage indices into a single set  $DI_j$  ( $j = 1, 2, 3, \dots, NE$ ) for  $NE$  structural elements, and 3) to assign damage to particular elements by classifying damage indices upon the confidence level of interest.

The elements are assigned to a damage class via a statistical-pattern-recognition technique that utilizes hypothesis testing (Kim and Stubbs 1995). The following statistical criteria are established for damage localization. For the given a set of DI results, the locations of damage are selected on the basis of a rejection of hypothesis in the statistical sense. The collection of values  $DI_j$  ( $j = 1, 2, 3, \dots, NE$ ) associated with each element and each neural networks set is treated as a random variable. In other words, the collection of the damage indices  $DI_j$  is treated as a sample population of damage indices (assuming the variable distributed normally). We first normalize the damage indices  $DI_j$  according to the standard rule.

$$Z_j = (DI_j - \mu_{DI}) / \sigma_{DI} \quad (7)$$

in which  $\mu_{DI}$  and  $\sigma_{DI}$  represent, respectively, the mean and standard deviation of the collection of  $DI_j$  values. The null hypothesis (i.e.  $H_0$ ) is taken to be that the structure is undamaged at the  $j$ th element and the alternate hypothesis (i.e.  $H_1$ ) is taken to be that the structure is damaged at the  $j$ th element. In assigning damage to a particular location, we utilize the following decision rule: (1) choose  $H_1$  if  $Z_j \geq z_o$ ; and (2) choose  $H_0$  if  $Z_j < z_o$ , where  $z_o$  is number which depends upon the confidence level of the localization test.

### 3. Numerical verification

Structural responses are dependent upon excitation forces, as described previously in Eq. (2). To produce the best output, neural networks should be trained by using excitation forces equivalent to the real ones applied to the structure. Although the impact forces can be measured, it may be difficult that the impact excitation patterns be equalized with the excitation patterns used for training neural network. For example, Fig. 3 shows three impact loads that were experimentally measured from impact hammer tests in the lab. These impact excitation patterns show different in their shapes, durations and intensities. In most real structures such as bridges or buildings, moreover, it is almost impossible to control excitation forces unless these structures are tested under the complete vacancy or traffic control. Since a loading pattern matching to real excitation is not possible unless it is measured.

In this proposed method, model uncertainty in neural networks may exist due to the difference between the excitation pattern selected for training neural networks (i.e. ‘Select  $N$  Loading Patterns’ for TNN in Fig. 2) and the excitation force applied for acquiring acceleration data to alarm the location of damage (i.e. ‘Acquire Accelerations from Target Structure’ for ADL in Fig. 2). Therefore, it is needed to evaluate the feasibility of the acceleration-based ANN method under the effect of the model uncertainty due to the variability of impulse excitation patterns used for training neural networks. We performed numerical tests on a simply supported beam by selecting several loading patterns for TNN process and also an excitation force (to acquire acceleration data) for ADL process.

#### 3.1. Test structure and numerical test setup

As described Fig. 4, a simply supported beam model, which consists of 9 nodes and 8 beam elements with equal size ( $L^{EL} = 0.28$  m), was selected and dynamic responses of the structure were obtained before and after a damaging episode. The geometrical properties of the model are as follows: the length  $L = 2.24$  m and moment of inertia  $I = 1.0856 \times 10^{-6}$  m. The material properties of the model are as follows: the elastic modulus  $E = 210$  GPa, Poisson’s ratio  $\nu = 0.3$  and mass density  $\rho = 7850$  kg/m<sup>3</sup>.

The geometry and numerical test lay-out with locations for acceleration acquisition and impact load are shown in Fig. 4(a) and 4(b), respectively. Two locations (i.e. Node 2 and Node 3 in Fig. 4(b)) were selected to acquire acceleration responses in the z-direction. Impact loads were applied at Node 7 and acceleration responses were analyzed by using commercial FEA software MIDAS/CIVIL. Sampling frequency was set to 10 kHz and total 16,384 discrete data were gathered from each test.

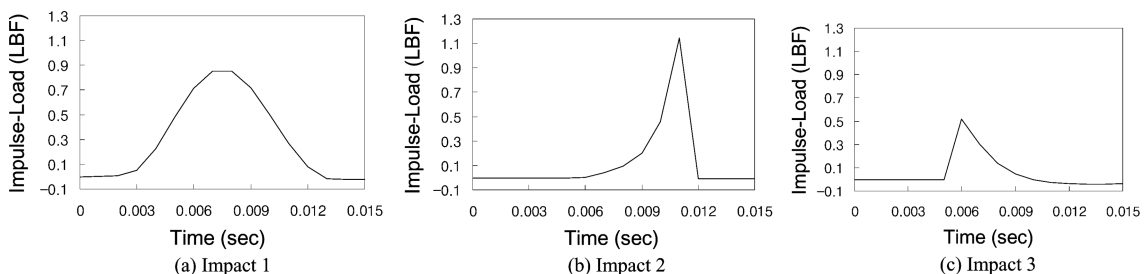


Fig. 3 Experimental excitation patterns measured from impact hammer test

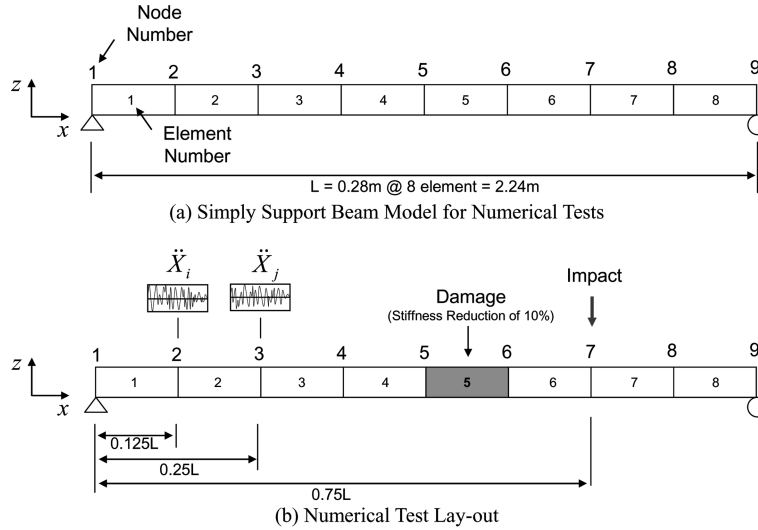


Fig. 4 Geometry and numerical test lay-out on simply supported beam

### 3.2. Training neural networks (TNN) for damage detection

As shown in Fig. 5, we selected eight loading patterns for TNN process. Each loading pattern creates an independent set of neural networks. As described in Fig. 5(a), Excitations 1-4 are triangular pulses with different durations (0~0.005sec, 0~0.01sec, and 0~0.02sec) and intensities (0.5% or 1.0% of beam weight). As described in Fig. 5(b), Excitations 5-8 are different in pulse shapes (triangular, right-triangular, rectangular, or delayed-rectangular) while duration 0~0.01 and intensity 1.0% are the same for all pulses.

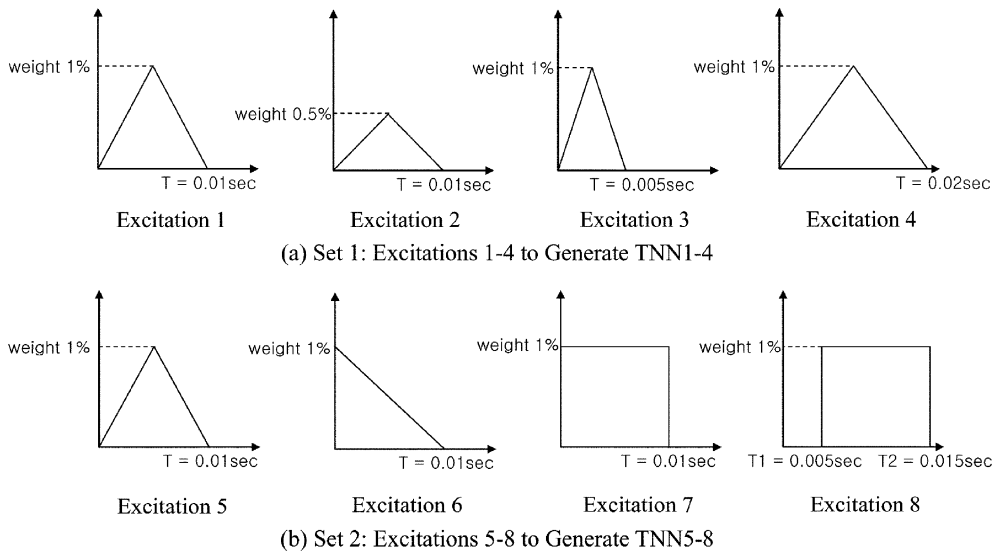


Fig. 5 Excitation patterns for training neural networks (TNN) for beam model

In order to train neural networks for damage detection, total 33 damage scenarios (including an intact case) were selected. For each element as a single damage location, the element stiffness loss (as described in Eq. 5) was simulated between 0.05 and 0.2 with a step size of 0.05 for each of 8 elements (i.e., 33 single damage cases). For each of the eight loading patterns, an independent TNN process was performed. That is, TNN 1 – TNN 8 were generated for their corresponding Excitation 1 – Excitation 8, respectively. Each TNN was generated by training for the 33 damage scenarios.

Selecting ANN architecture depends on the application domain and is usually determined by trial and error. In this study, each neural network (i.e. any of TNN 1 – 8) consisted of three layers (as shown in Fig. 1). The number of nodes for input layer was selected as 50 by trial and error by considering computational time and efficiency of computer memory. A good guess for the number of hidden neurons would be to put an average of the number of input and output neurons. Another possibility would be to make the hidden layer of the same size as either the input or the output layer (Barai and Pandey, 1995). In this study, we made the hidden layer of the same size as the input layer (i.e. 50 nodes). For the number of output neurons, we selected 8 units of element stiffness indices which were allocated to 8 elements of the beam model. The sigmoid function (which is recommended in most of back propagation applications) was used as the activation function. For training parameters, we set learning rate 0.3, momentum constant 0.9, error tolerance 0.0001, and epoch number 200. Also, the mean-squared performance function was used to measure the network's performance according to the mean of squared errors.

In the input layer, the 50 units of acceleration features are corresponding to the first 50 values of cross-covariance-ratios between intact and damaged state. Either intact or damaged state, cross-covariance signals were obtained from two acceleration signals  $\ddot{X}_i$  and  $\ddot{X}_j$  (i.e. Node 2 and Node 3 in Fig. 4). For the case of Excitation 1, Fig. 6 shows those two acceleration signals  $\ddot{X}_i$  and  $\ddot{X}_j$  and their cross-covariance function  $\rho_{\ddot{X}_i, \ddot{X}_j}$  obtained from the test model in intact state. In additional, Fig. 7 shows cross-covariance-ratios of the first 50 signal-data between intact and damaged states for 1) different levels of damage and 2) different locations of damage. The results show that the cross-covariance-ratios are sensitive to the location of damage as much as the amount of damage.

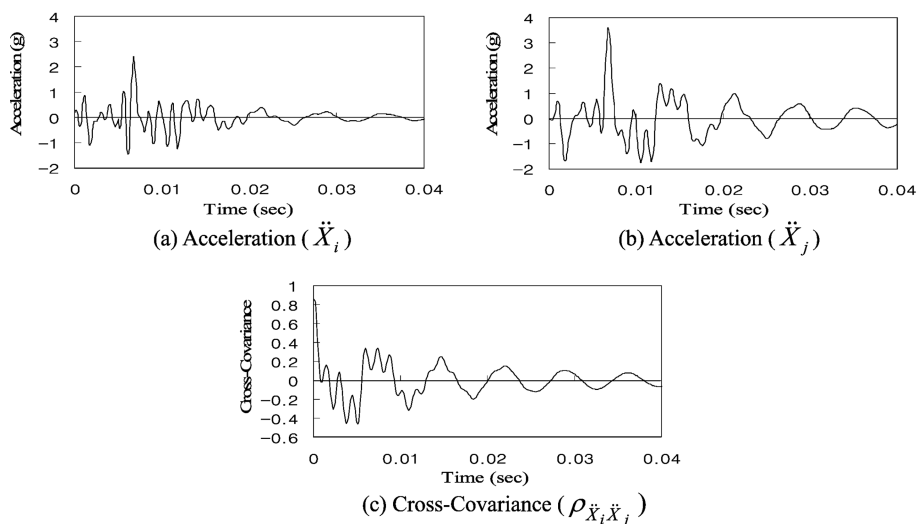


Fig. 6 Two acceleration signals and their cross-covariance function for beam model

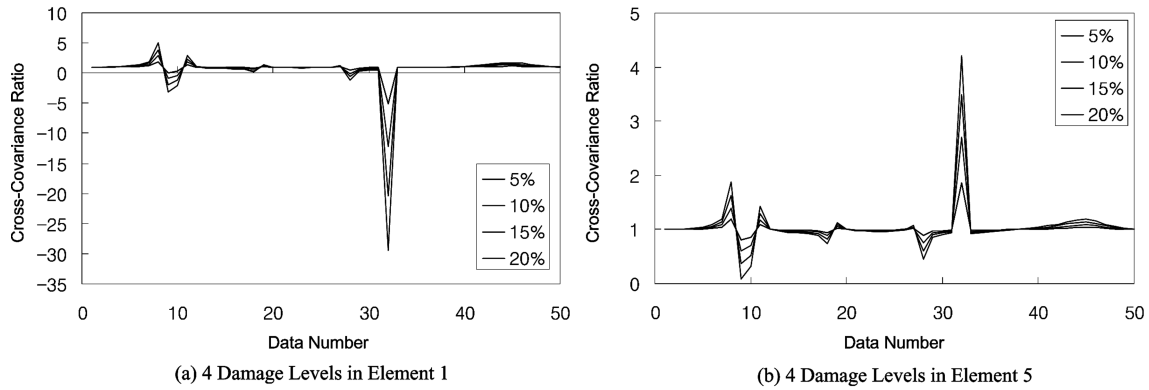


Fig. 7 Cross-covariance-ratios between intact and damage states

### 3.3. Alarming damage location (ADL) using neural network in numerical test

Damage was introduced by stiffness reduction of 10 percent to Element 5 of the test structure, as shown in Fig. 4. Accelerations were obtained from Node 2 ( $x/L = 0.125$ ) and Node 3 ( $x/L = 0.25$ ), which are equivalent to locations used for training neural networks. For alarming damage location (ADL), triangular pulse with 0~0.01 sec duration and pulse intensity of 1.0 percent of beam weight, which is the same as Excitation 1 in Fig. 5, was applied to the beam model to acquire acceleration data. As described previously, initial 50 cross-covariance ratios between intact and damaged state were computed from two acceleration signals (i.e.  $\ddot{X}_i$  and  $\ddot{X}_j$  in Fig. 4) obtained from the beam model.

From each TNN, stiffness indices were estimated for the 8 elements of the test structure. Total eight independent sets of stiffness indices were computed from TNN 1 – TNN 8, respectively. In order to examine the variability of the damage detection results on the impact excitation parameters (i.e., pulse-shape, duration and intensity), we performed two sets of tests as follows: Set 1 using first four neural networks TNN 1 – TNN 4 as listed in Table 1 and Set 2 using remaining four neural networks TNN 5 – TNN 8 as listed in Table 2.

Table 1 shows the stiffness indices estimated by using TNN 1 – TNN 4 (i.e. Set 1), which are triangular pulses with different durations and intensities. By TNN 1 when the duration and intensity are the same for both TNN and ADL, the stiffness indices were correctly identified (indicative to Element 5 with 10% stiffness-loss). By TNN 2 when the duration is the same but the intensity is different, the stiffness indices were accurately estimated with very small error. Since we used cross-covariance instead of acceleration data, the pulse intensity had the minor effect on the result of damage detection. By TNN 3 or TNN 4 when the intensity is the same but the duration is different (half or double), the stiffness indices were estimated with relative low accuracy but indicative to the damaged element with the minimum element stiffness index. That is, the difference in time-duration leads to negative effect in the damage detection and this may lead false-alarmed locations.

Also, Table 2 shows the stiffness indices estimated by using TNN 5 – TNN 8 (i.e. Set 2) which are different in pulse shapes but with the same duration and intensity. In TNN 5 when the pulse shapes are the same for both TNN and ADL, the stiffness indices were correctly identified. In TNN 6 – TNN 8 when the pulse shapes are different for TNN and ADL, the stiffness indices were estimated with relatively low accuracy but indicative to the damaged element. It is note that the difference in pulse shape has relatively large impact on the accuracy of damage detection this may lead false-alarmed

Table 1 Stiffness indices estimated by Set 1 (TNN 1 – TNN 4)

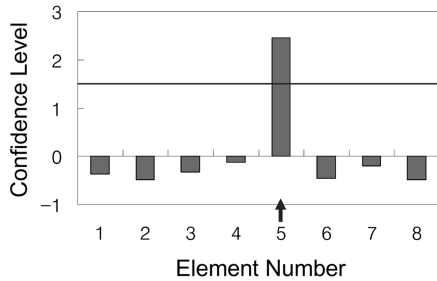
Case	Excitation pattern for TNN	Excitation pattern for ADL	Element stiffness indices by each TNN
1			
2			
3			
4			

locations.

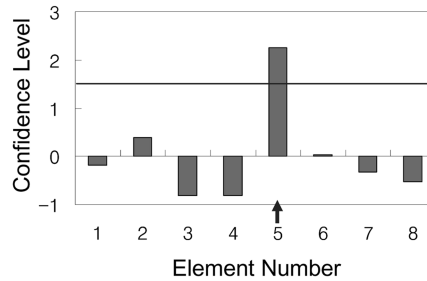
Finally, we utilized the statistical damage classification process, which is described in the previous section, to detect damage under the uncertainty related to the completeness of neural networks. On assuming the stiffness indices distributed normally, normalized damage indices were generated in accordance with Eq. (7) (note that the analysis indicates that the damage indices approximately fit into normal distribution by excluding the damaged elements which are the special causes). The confidence level for the localization corresponded to  $z_0 = 1.5$ . This criterion corresponds to a one-tailed test at a confidence level of 93.3%. The damage localization results of Set 1 and Set 2 are shown in Figs. 8(a) and 8(b), respectively. Both for Set 1 and Set 2, Element 5 was predicted where damage was inflicted.

Table 2 Stiffness indices estimated by Set 2 (TNN 5 – TNN 8)

Case	Excitation pattern for TNN	Excitation pattern for ADL	Element stiffness indices by each TNN
5			
6			
7			
8			



(a) Result by Set 1 (TNN 1-TNN 4)



(b) Result by Set 2 (TNN 5-TNN 8)

Fig. 8 Damage localization results for beam model

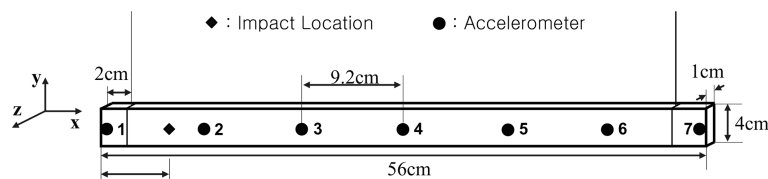
## 4. Experimental verification

### 4.1. Test structure and experimental setup

Experiments were performed to evaluate the feasibility and the practicality of the acceleration-based ANN algorithm. As described in Fig. 9, a free-free, uniform, aluminum beam, which has simple geometry and boundary condition, and low damping property, was selected and dynamic responses of the structure were measured before and after damaging episodes. This structure was used to evaluate the *algorithm* since structural parameters of its baseline model was relatively easy to identify compared to other beam geometries and material properties. The geometrical properties of the test structure are as follows: the length  $L = 56$  cm and the rectangular cross-section  $t \times H = 1 \text{ cm} \times 4 \text{ cm}$ . The material properties of the test structure are as follows: the elastic modulus  $E = 70 \text{ GPa}$ , Poisson's ratio  $\nu = 0.33$ , and mass density  $2700 \text{ kg/m}^3$ .

The geometry and experimental layout with locations and arrangements of the accelerometers are shown in Fig. 9. Seven accelerometers were selected to measure the motion of the structure in the  $z$ -direction (i.e. the vertical direction to sense out-of-plane motions) and equally distanced (i.e.  $9.2$  cm) along the longitudinal direction. Impulse loads were applied by hand, but not controlled, to a location  $6$  cm distanced from the left edge by using a Dytran impulse hammer 5801A with force sensor. Acceleration responses were sensed by using Dytran 3101BG miniature accelerometers mounted along the center line. A data acquisition system which included 16 channels National Instrument PXI-4472 DAQ, PXI-8186 controller, and LabVIEW was set up to measure signals from the accelerometers. Sampling frequency was set to  $8.0$  kHz and total  $8,450$  discrete data were acquired from each measure.

Accelerations were measured from Sensor 3 ( $x/L = 0.32$ ) and Sensor 4 ( $x/L = 0.5$ ) before and after damage. Figure 10 shows acceleration signals measured from the two sensors and their cross-covariance function, respectively. The impulse was applied to a location  $6$  cm distanced from the left edge by hand-hammering but not controlled. To update the baseline model, modal characteristics of the test beam were extracted from measured acceleration-response signals by using frequency-domain



(a) Geometry of Free-Free Beam



(b) Experimental Layout

Fig. 9 Experimental setup on free-free beam

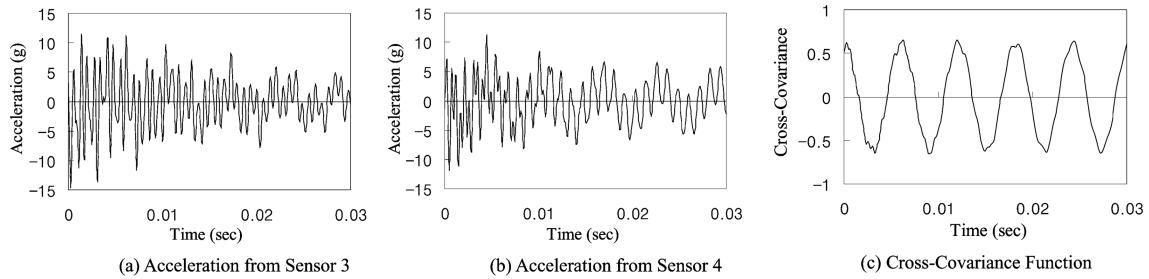


Fig. 10 Two measured acceleration signals and cross-covariance function

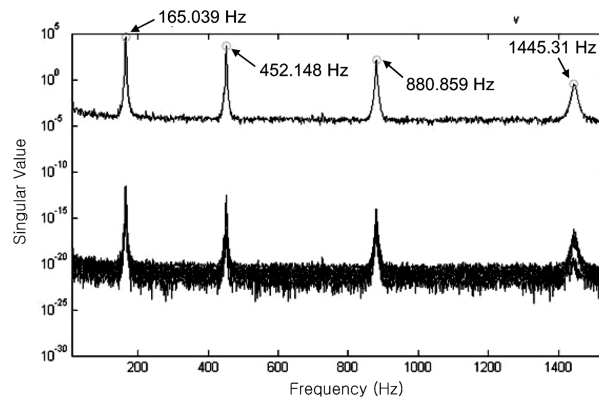


Fig. 11 Singular values of PSD matrix of acceleration signals

Table 3 Natural frequencies of free-free beams

Mode	Natural frequency		
	Experiment (Hz)	FE Model (Hz)	Error (%)
1	165.039	165.218	0.11
2	452.148	453.630	0.33
3	880.859	888.845	0.91
4	1445.315	1463.376	1.25

decomposition (FDD) technique (Yi and Yun, 2004; Brinker, *et al.* 2001). Fig. 11 shows the singular values (and the corresponding resonant frequencies) calculated by singular value decomposition of power spectral density (PSD) matrix. The figure identified the natural frequencies of the initial four modes as listed in Table 3.

#### 4.2. Training neural networks (TNN) for damage detection

In order to train neural networks and further to utilize those for damage detection, we selected a baseline free-free beam model which consists of 12 beam elements with equal size ( $L^{EL} = 4.6$  cm) and with uniform bending rigidity ( $EI = 233.3$  N·m<sup>2</sup>). In order to identify the representation of the baseline model, natural frequencies and mode-shapes of the baseline model were compared to the corresponding experimental results. As shown in Fig. 12, mode shapes of the four modes were accurately identified with very high modal-assurance-criterion (MAC) values between the experimental structure and FE

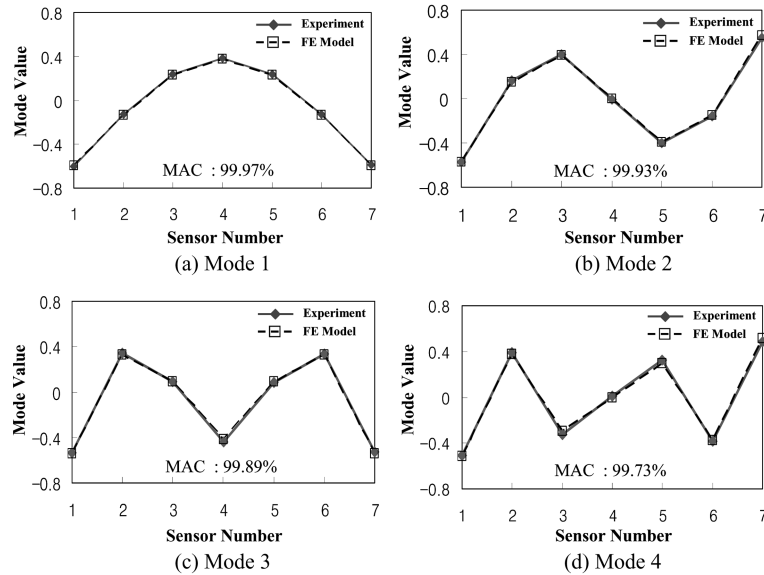


Fig. 12 Comparison of mode shapes: experiment vs FE model

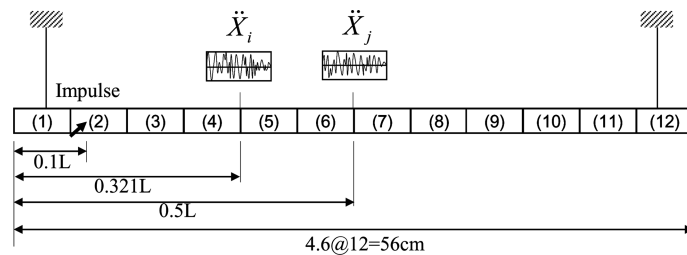


Fig. 13 Lay-out of acceleration signal acquisition in baseline model

model. As also listed in Table 3, all natural frequencies were accurately identified with relatively low errors between the experimental structure and the FE model. Note that damping properties were not considered in this study. In case of more complex structures with high damping properties, however, the system identification of the baseline model should be performed in a systematic way to guarantee that all modal parameters including damping properties of the model match with those of the structure.

Fig. 13 shows the lay-out of acceleration signal acquisition in the baseline model. The numerical impulse-response tests were performed in the following ways. Firstly, we selected a set of excitation types to simulate unknown impulse loadings. As described previously, the excitation pattern of an impulse can be characterized by its shape, time-delay, duration, and intensity. Due to the lack of prior knowledge on the real impulse measurements, we should rely on a set of potential excitation patterns. As shown in Fig. 14, four excitation types were selected: (1) Excitation 1 – triangular pulse with 0~0.01 sec duration, (2) Excitation 2 – right triangular pulse with 0~0.01 sec duration, (3) Excitation 3 – rectangular pulse with 0~0.01 sec duration, and (4) Excitation 4 – rectangular pulse with 0.005~0.015 sec duration. Pulse intensity was set to 5 percent of self-weight of the test beam.

Secondly, the selected excitation impulses were applied to the location  $0.1L$  and accelerations were obtained from the locations  $0.3214L$  (i.e. node 5) and  $0.5L$  (i.e. Node 7). Sampling frequency was set

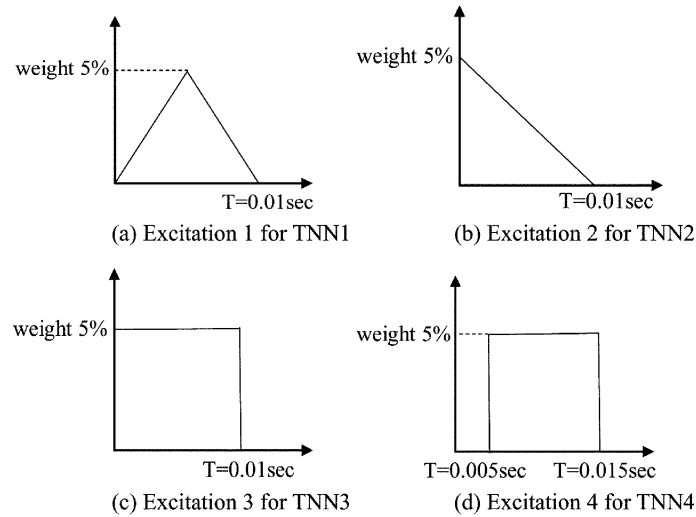


Fig. 14 Four excitation patterns for training neural networks (TNN 1 – TNN 4)

to 8 kHz and total 8,450 discrete acceleration data were numerically analyzed for each measure. Finally, damage scenarios were selected to train neural networks for damage detection. Total 127 scenarios were selected. For each element as a single damage location, the element stiffness loss (as described in Eq. 5) was simulated between 0.1 and 0.5 with a step size of 0.1 for each of 12 elements (i.e. 61 single-damage cases). For two elements as dual damage locations, the element stiffness losses were only simulated for a limited combination of 0.1 for both elements (i.e. 66 dual-damage cases). Note that total number of dual-damage cases are extended to 25 times as of the 66 cases if all possible combinations of the element stiffness (i.e. 0.1, 0.2, ..., 0.5) are considered.

Four sets of training neural networks (TNN 1 – TNN 4) were generated for the 4 excitation patterns in which each TNN was trained for the 127 damage scenarios including the intact state. Therefore, totally 505 training patterns were considered for damage detection in the test structure. In this study, each neural network (i.e. any of TNN 1 – 4) consisted of three layers (as illustrated in Fig. 1). Fifty (50) nodes for input layer and the same 50 nodes for hidden layer were selected. For the number of output neurons, we selected 12 units of element stiffness indices, each of which was allocated to each of 12 beam elements. The sigmoid function was used as the activation function. For training parameters, we set learning rate 0.3, momentum constant 0.9, error tolerance 0.0001, and epoch number 200. Also, the mean-squared performance function was used to measure the network's performance according to the mean of squared errors.

In the input layer, the 50 units of acceleration features are corresponding to the first 50 values of cross-covariance-ratios between intact and damaged state. Either intact or damaged state, cross-covariance signals were obtained from two acceleration signals (i.e. from  $\ddot{X}_i$  and  $\ddot{X}_j$  shown in Fig. 11). Note that the two acceleration signals and their cross-covariance signal obtained from the baseline model are similar as shown in Fig. 6.

### 4.3. Alarming damage location (ADL) using neural networks

As shown in Fig. 15, damage was inflicted by sawing cuts at two different locations of the beam. Three different scenarios of damage were introduced as follows: (1) Damage Case 1 – a single damage

at  $x/L = 0.464$  (26cm distanced from the left edge) with severity  $a/t = 0.25$  (0.25 mm thick), (2) Damage Case 2 – a single damage at  $x/L = 0.464$  with  $a/t = 0.5$ , and (3) Damage Case 3 – two damages at  $x/L = 0.464$  and  $x/L = 0.939$  (3.4 cm distance from the right edge) with  $a/t = 0.5$  and  $a/t = 0.25$ , respectively.

Accelerations were measured from Sensor 3 ( $x/L = 0.32$ ) and Sensor 4 ( $x/L = 0.5$ ) before and after each damage scenario. For each damage case, cross-covariance ratios were computed from cross-covariance signals measured before and after damage. Initial 50 cross-covariance ratios were input into the four sets of trained neural networks (TNN 1 – TNN 4). From each TNN, stiffness indices were estimated for the 12 elements of the test structure. That is, four independent sets of stiffness indices were computed from TNN 1 – TNN 4, respectively.

Figs. 16-18 show the estimated stiffness indices of the test structure for the three damage cases, respectively. The elements 6 and 12 are corresponding to the real cut locations  $x/L = 0.464$  and  $x/L = 0.939$  in the test beam, respectively. For each damage case, element stiffness indices were estimated from the four sets of neural networks (TNN 1 – TNN 4), respectively. In single damage cases (Damage Case 1 and Damage Case 2), as shown in Figs. 16-17, the real damage was indicated with the minimum index but also several other locations were indicated with remarkable stiffness-loss. In dual damage case (Damage Case 3), as shown in Fig. 18, the stiffness-loss was indicated at several locations including the correct one. Finally, damage was localized by computing damage indices according to Eq. (6). On assuming the stiffness indices distributed normally, normalized damage indices were calculated from Eq. (7). The confidence level for the localization was  $z_0 = 1.5$ , which corresponds to the

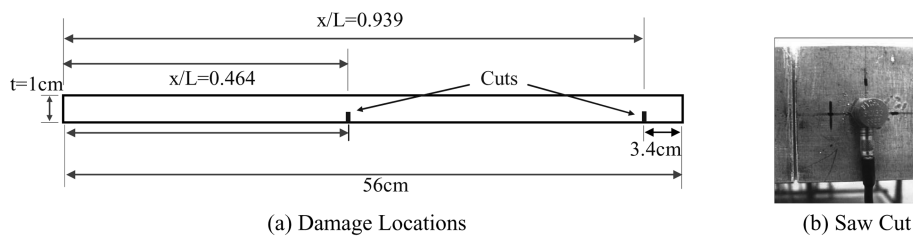


Fig. 15 Damage inflicted in test structure

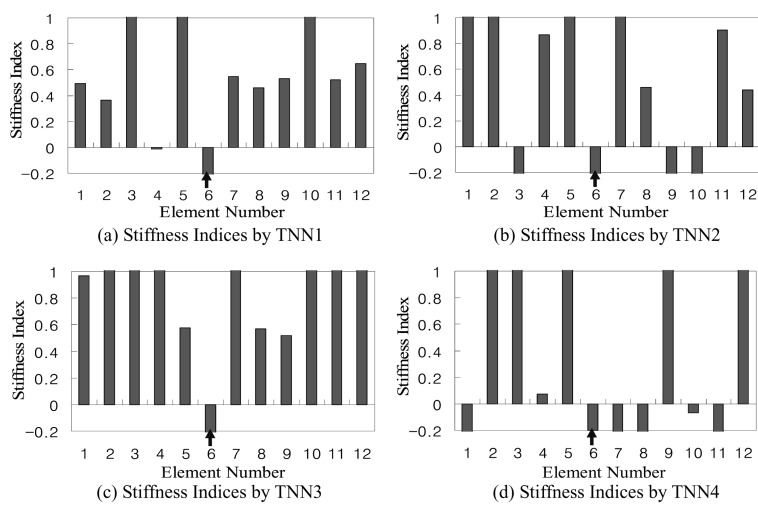


Fig. 16 Estimated stiffness indices for Damage Case 1

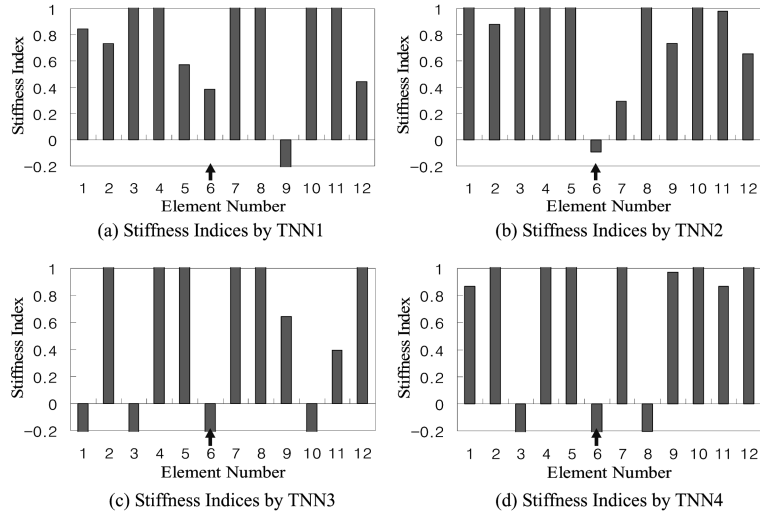


Fig. 17 Estimated stiffness indices for Damage Case 2

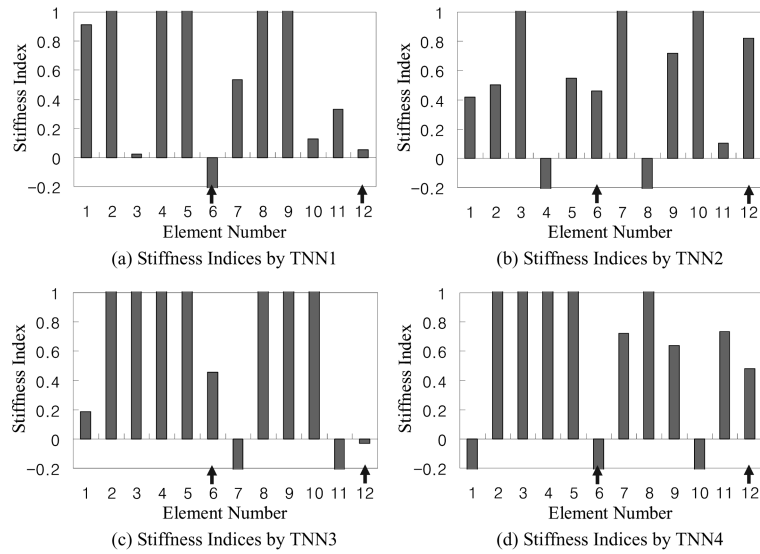


Fig. 18 Estimated stiffness indices for Damage Case 3

confidence level of 93.3%.

The damage localization results for the three damage cases are shown in Fig. 19. In Damage Case 1 and 2, the correct element 6 was predicted, which is identical to the damaged location. In Damage Case 3, elements 1 and 6 were predicted, in which the first one is false-alarm (note that element 1 is the opposite symmetric location of element 12 where damaged) and the second one is correct. Also, by setting the confidence level  $z_0 = 1.3$  which gives 90.3% confidence level, element 11 could be also predicted, which shows about 8% localization error. This inaccuracy is mostly due to the limited number of training patterns for dual damage cases, as described previously.

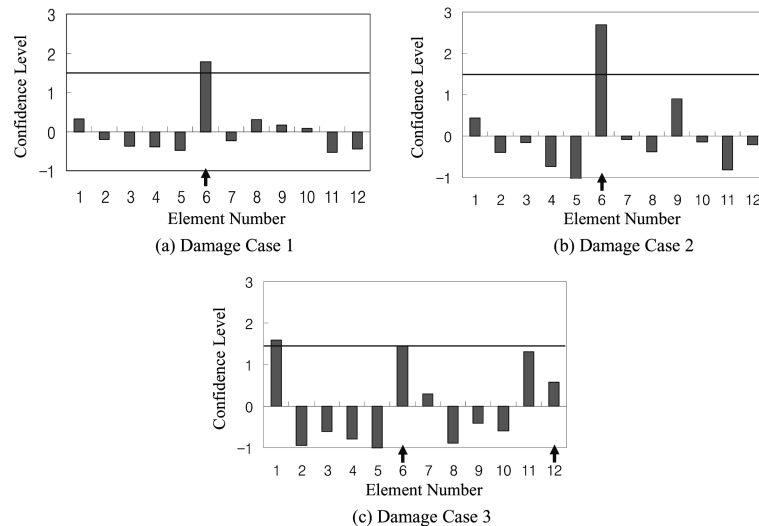


Fig. 19 Damage localization results for test structure

## 5. Summary and conclusions

Several problems should be resolved for the realization of the on-line, vibration-based damage detection using artificial neural networks (ANN). One of the main obstacles is that signal process and modal analysis need time-consuming off-line works that depend on the number of sensors involved and the amount of signals recorded. Also, errors in modal features used for the input to neural networks have effects on the accuracy of damage detection. In this study, we developed an ANN-based algorithm that uses real-time acceleration features measured from a limited number of sensors, without any further frequency-domain data-process, to identify the changes in structural conditions. Firstly, theoretical backgrounds were described. The problem addressed in this paper was defined as the stochastic process. Also, an ANN-algorithm using output-only acceleration responses was newly designed for damage detection in real time. As the feature representing the structural condition, we selected the cross-covariance function of two acceleration signals measured at two different locations. By means of the acceleration features, multiple neural networks were trained for a series of potential loading patterns and damage scenarios of the target structure for which its actual loading history and structural conditions were unknown.

The feasibility of the proposed method was evaluated from numerical tests on simply supported beams under the effect of model uncertainty due to the difference in impulse excitation properties (i.e. pulse shape, duration and intensity) between the process for training neural networks (TNN) and the process for alarming damage location (ADL). Firstly, we estimated the stiffness indices of the beam model as follows: (1) When the pulse shape, duration and intensity are the same for both TNN and ADL, the stiffness indices were correctly identified; (2) When the pulse shape and duration are the same but the intensities are different for TNN and ADL, the stiffness indices were estimated with relatively high accuracy; (3) When the pulse shape and intensity are the same but the durations are different for TNN and ADL, the stiffness indices were estimated with relatively low accuracy (but indicative to the damaged location); and (4) When the pulse shapes are different while the intensity and

duration remain the same, the stiffness indices were estimated with relatively low accuracy (but indicative to the damaged location). Secondly, we detected the location of damage by implementing the statistical damage classification process into the estimated results of damage indices obtained from multiple TNNs. Damage was correctly located with a confidence level of 93.3%.

The practicality of the proposed method was evaluated from laboratory-model tests on a free-free, aluminum beam for which its actual loading histories were unknown. Four (4) excitation types and 127 damage scenarios were selected to train four independent sets of neural networks for a baseline model with 12 beam elements. Initial 50 acceleration data measured from two accelerometers were input into the neural networks and stiffness indices of the 12 elements of the test structure were estimated as the output. From the damage detection process, single-damage locations were predicted correctly but dual-damage locations were predicted with relatively high localization errors.

Future study should be focused on extensively assessing the accuracy of the FE model and its effect on the accuracy of damage detection before this method would be applied to full-scale structures. The quality of impulse loading and the representation of baseline model for training neural networks should be assessed more rigorously to deal with some real-situation parameters such as damping properties and boundary conditions.

## Acknowledgements

This study was supported by Smart Infra-Structure Technology Center (SISTeC) under the research grant (R11-2002-101-03002-0) of Korea Science and Engineering Foundation (KOSEF). The second author was financially supported by Brain Korea 21 program in year 2007.

## References

- Barai, S. V. and Pandey, P. C. (1995), "Vibration signature analysis using artificial neural networks", *ASCE, J. Comput. Civ. Eng.*, **9**(4), 259-265.
- Bendat, J. S. and Piersol, A. G. (1991), *Random Data Analysis and Measurement Procedures*, John Wiley & Sons, Singapore.
- Brinker, R., Zhang, L and Andersen, P. (2001), "Modal identification of output-only systems using frequency domain decomposition", *Smart Mater. Struct.*, **10**, 441-445.
- Catbas, F. N. and Aktan, A. M. (2002), "Condition and damage assessment: issues and some promising indices", *ASCE, J. Struct. Eng.*, **128**(8), 1026-1036.
- Chen, Y. and Feng, M. Q. (2005), "Condition assessment of bridge sub-structure by vibration monitoring", *2<sup>nd</sup> International Workshop on Advanced Smart Materials and Smart Structures Technology*, Co-edited by C.B. Yun and B. F. Spencer, Gyeongju, Korea, 21-24 July, 651-676.
- Doebling, S. W., Farrar, C. R. and Prime, M. B. (1998), "A summary review of vibration-based damage identification methods", *Shock Vib. Digest*, **30**(2), 91-105.
- Gao, Y. and Spencer, B. F. (2002), "Damage localization under ambient vibration using changes in flexibility", *J. Earthq. Eng. Earthq. Vib.*, **1**(1), 136-144.
- Hao, H. and Xia, Y. (2002), "Vibration-based damage detection of structures by genetic algorithm", *J. Comput. Civ. Eng.*, **16**(3), 222-229.
- Jang, C. and Imregun, M. (2001), "Structural damage detection using artificial neural networks and measured FRF data reduced via principal component projection", *J. Sound. Vib.*, **242**(5), 813-827.
- Kim, J. T. and Stubbs, N. (1995), "Model uncertainty impact and damage-detection accuracy in plate-girder", *ASCE, J. Struct. Eng.*, **121**(10), 1409-1417.

- Kim, J. T., Ryu, Y. S., Cho, H. M. and Stubbs, N. (2003), "Damage identification in beam-type structures: frequency-based method vs mode-shape-based method", *Eng. Struct.*, **25**, 57-67.
- Kim, J. T., Park, J. H., Do, H. S. and Lee, Y. H. (2006), "Real-time damage monitoring using output-only acceleration data", *Asia-Pacific Workshop on Structural Health Monitoring*, Edited by A. Mita at Keio Univ., Yokohama, Japan, 2-4 December, 404-411.
- Kim, J. T., Park, J. H., Yoon, H. S. and Yi, J. H. (2007), "Vibration-based damage detection in beams using genetic algorithms", *Smart Struct. Sys.*, **3**(3), 263-280.
- Lee, I. W., Oh, J. W., Park, S. K. and Kim, J. T. (1999), "Damage assessment of steel box-girder bridge using neural networks", *J. Korean Society of Steel Construction*, **11**(1), 79-88.
- Lee, J. J., Lee, J. W., Yi, J. H., Yun, C. B. and Jung, J. Y. (2005), "Neural networks-based damage detection for bridges considering errors in baseline finite element models", *J. Sound. Vib.*, **280**(3), 555-578.
- Ni, Y. Q., Wang, B. S. and Ko, J. M. (2002), "Constructing input vectors to neural networks for structural damage identification", *Smart Mater. Struct.*, **11**, 825-833.
- Szewczyk, Z. P. and Hajela, P. (1994), "Damage detection in structures based on feature-sensitive neural networks", *ASCE, J. Comput. Civ. Eng.*, **8**(2), 163-178.
- Wu, X., Ghaboussi, J. and Garret Jr., J. H. (2001), "Use of neural networks in detection of structural damage", *Comput. Struct.*, **42**(4), 649-659.
- Yi, J. H. and Yun, C. B. (2004), "Comparative study on modal identification methods using output-only information", *Struct. Eng. Mech.*, **17**(3-4), 445-466.
- Yang, J. N., Pan, S. and Huang, H. (2007), "An adaptive extended Kalman filter for structural damage identifications II: unknown inputs", *Struct. Control. Health Monitoring*, **14**(3), 497-521.
- Yun, C. B. and Bhang, E. Y. (2001), "Joint damage assessment of Framed Structures using Neural Networks Technique", *Eng. Struct.*, **23**(5), 425-435.